Available online at www.sciencedirect.com

SciVerse ScienceDirect

Ceramics International 38 (2012) 1371–1380

CERAMICS INTERNATIONAL

www.elsevier.com/locate/ceramint

Influence of sintering temperature and holding time on the densification, phase transformation, microstructure and properties of hot pressing WC–40 vol.%Al_2O_3 composites

Haixia Qu [a], Shigen Zhu [a,b,*], Qian Li [a], Chenxin Ouyang [a,b]

[a] College of Mechanical Engineering, Engineering Research Center of Advanced Textile Machinery, Ministry of Education, Donghua University, Shanghai 201620, PR China

[b] College of Material Science and Engineering, Donghua University, Shanghai 201620, PR China

Received 24 May 2011; received in revised form 4 September 2011; accepted 6 September 2011
Available online 14 September 2011

Abstract

WC–40 vol.%Al_2O_3 composites were prepared by high energy ball milling followed by hot pressing. The tungsten carbide (WC) and commercial alumina (Al_2O_3) powders composed of amorphous Al_2O_3, boehmite (AlOOH) and χ-Al_2O_3 were used as the starting materials. The phase transformation during sintering, the influence of sintering temperature and holding time on the densification, microstructure, Vickers hardness and fracture toughness and the toughening effects of WC–40 vol.%Al_2O_3 composites were investigated. The results showed that the amorphous Al_2O_3, AlOOH and χ-Al_2O_3 were transformed to α-Al_2O_3 completely during the sintering process. With the increasing sintering temperature and holding time, the relative density increased and both the Vickers hardness and fracture toughness increased initially to the maximum values and then decreased. When the as milled powders were hot pressed at 1540 °C for 90 min, a relative density of 97.98% and a maximum hardness of 18.65 GPa with an excellent fracture toughness of 10.43 MPa $m^{1/2}$ of WC–40 vol.%Al_2O_3 composites were obtained.

Keywords: A. Hot-pressing; B. Microstructure-final; C. Mechanical properties; D. WC–Al_2O_3 composites

1. Introduction

Among the hard alloys, tungsten carbide (WC) has achieved significant scientific and technological attention for use in cutting tools, drilling and mining equipments due to its excellent properties, such as high melting point, superior hardness and strength, low friction coefficient, good electrical conductivity and intrinsic resistance to oxidation and corrosion at high temperature. However, the relatively low value of fracture toughness, poor ductility and shock resistance of monolithic WC limits its applicability under severe conditions such as for high speed cutting tools [1]. Metallic cobalt (Co) is usually used as binder material to improve several mechanical properties of WC. Embedding the WC grains, the naturally ductile Co metal serves to offset the characteristic brittle behavior of WC ceramic, thus raise its toughness and durability [2,3]. Since Co has low melting point, when the WC–Co composites are used as cutting tools, the Co phase will be oxidized during the cutting process, because of the raised temperature induced by the increase of cutting speed. In addition, Co has other shortcomings, namely, poor corrosion resistance, high cost and environmental toxicity, which limit the use of WC–Co materials in industrial applications [4]. In the past few decades, Co binder was replaced by Ni [5], Fe [6], TiC [7], ZrO_2 [8], Fe_3Cl [9], MgO [10,11], etc., significant researches efforts have been focused on developing WC with none metallic binders.

Among them, Malek et al. [8] consolidated WC–ZrO_2 composites combining a hardness of 25.48 GPa with a fracture toughness of 6 MPa $m^{1/2}$ using spark plasma sintering. Hot pressing sintered WC–MgO composites with a Vickers hardness of 15.43 GPa and a fracture toughness of 9.58 MPa $m^{1/2}$ were consolidated by Ma et al. [12]. Al_2O_3 is another refractory oxide with low price, superior hardness, high

* Corresponding author at: College of Mechanical Engineering, Engineering Research Center of Advanced Textile Machinery, Ministry of Education, Donghua University, Shanghai 201620, PR China. Tel.: +86 21 6779 2813; fax: +86 21 6779 2813.
E-mail address: sgzhu@dhu.edu.cn (S. Zhu).

0272-8842/$36.00
doi:10.1016/j.ceramint.2011.09.016

resistance to oxidation and corrosion at high temperature. As the melting point of Al_2O_3 is lower than that of ZrO_2 and MgO, the sintering temperature of WC–Al_2O_3 will be lower than that of WC–ZrO_2 and WC–MgO composites. In addition, Al_2O_3 is inexpensive compared to Co, ZrO_2 and MgO, indicating that the WC–Al_2O_3 composites will be lighter, much more economical and suitable for industrial application.

Recently, we have attempted to synthesis Al_2O_3 particulate toughened WC matrix composites using hot pressing method. Thermodynamic consideration of reaction between WC and Al_2O_3 reveals that WC and Al_2O_3 have good adopting characteristics, as there is no reaction and no interface phase between them. The thermal expansion coefficients of Al_2O_3 and WC are $8.8 \times 10^{-6}\,K^{-1}$ and $3.84 \times 10^{-6}\,K^{-1}$, respectively [13]. Although they are of the same magnitude order of 10^{-6}, the mismatch between them would create residual stresses and induce complex residual stress field on the WC/Al_2O_3 interfaces to influence the mechanical properties of the samples.

Some previous studies investigate the synthesis of WC–Al_2O_3 powders. Sherif and El-Eskandarany [14] synthesized nanocomposite WC–Al_2O_3 powders from WO_3, Al and graphite by high-energy reactive milling and subsequently consolidated the powders by plasma-activated sintering. Pallone et al. [15] investigate the synthesis of WC–Al_2O_3 composites by high-energy reactive milling, adding Al_2O_3 and C to obtain Al_2O_3–WC composites. The effect of aluminum content on the behavior of mechanochemical reactions and the control of carbon loss during synthesis of WC–Al_2O_3 powders were studied by Sakaki et al. [16,17]. Some studies are carried out to investigate the sintering of WC–α–Al_2O_3 composites. Endo and Ueki [18] obtained WC–Al_2O_3 composites by both hot pressing and pressureless sintering. The sintering and properties of Al_2O_3–WC composite with a substantial WC content up to 80 vol.% were studied by Huang et al. [19].

Despite numerous papers on the synthesis and characterization of WC–Al_2O_3 powders and WC–Al_2O_3 composites with α-Al_2O_3 as the starting materials, little information is available on the sintering parameters and phase transformation process of WC–Al_2O_3 composites with commercial Al_2O_3 composed of AlOOH, χ-Al_2O_3 and amorphous Al_2O_3 as the starting materials. The aims of present work are to synthesis the commercial Al_2O_3 particulate toughened WC matrix composites by hot pressing method, and investigate the effects of sintering temperature and holding time on the densification, microstructure evolution and room temperature properties of consolidated bulk. Meanwhile, the process of phase transformation during the sintering and its effect on the toughening of WC–40 vol.% Al_2O_3 composites are discussed.

2. Experimental procedure

Commercial powders of WC (74 μm, 99% purity, Sinopharm Chemical Reagent Co. Ltd.) and Al_2O_3 (composed of AlOOH, χ-Al_2O_3 and amorphous Al_2O_3; 150 μm, Sinopharm Chemical Reagent Co. Ltd.) were mixed and ball milled using a QM-1SP4 planetary ball milling machine under argon gas atmosphere for 50 h. The ball to powder weight radio was 10:1 and the rotation speed of the mill was 350 revolutions per minute (rpm). Both the vial and milling balls (10 mm in diameter) were made of cemented carbide materials.

The as milled powders were cold pressed and the shrinkage of the green compact were studied in a dilatometer (DIL402C Netzsch) up to 1500 °C at a heating rate of 5 °C/min with N_2 flow at 50 ml/min to study the densification process and determine the range of sintering temperature. Then the as milled powders were hot pressed using a vacuum hot pressing furnace (ZT-40-20YB, Shanghai Chen Hua Electric Furnace Co. Ltd.) in the range of 1440–1740 °C under a pressure of 39.6 MPa (applied already from the start) in a vacuum (about 1.3×10^{-1} Pa) atmosphere for 60 min, 90 min and 120 min, respectively. The heating rate of the hot pressing was 10 °C/min. Carbonic paper with a thickness of 0.2 mm was used to prevent adhesion between powders and the die. The thermoelectric couple and infrared thermometer were selected to measure the temperature, located in the surface of the mold.

The phase identification of the as milled powders and sintered samples were investigated by X-ray diffraction (XRD) using a D/max-2550PC (Rigaku Co., Japan) X-ray diffractometer with a Cu K_α radiation ($\lambda = 0.15418$ nm) at 400 kV and 200 mA. The microstructure of the as milled powders and sintered samples were characterized by S-4800 (Hitachi Co., Japan) field emission scanning electron microscope (FE-SEM). The polished and etched samples were characterized by JSM-5600LV (JEOL Co., Japan) scanning electron microscope (SEM). The JEOL JEM-2100F Transmission Electron Microscope (TEM) was also used to investigate morphologies of the powders. The density of the sintered samples was measured using water immersion method in accordance with Archimedes' principle. The hardness of sintered specimens (the average of 10 indentations) was determined using a HVS-50Z Vickers indenter with a load of 30 kg and a dwell time of 10 s. The crack shapes of the specimen determined by repeated surface polishing were confirmed to be Palmqvist crack pattern and in accordance with the Shetty's model, so the fracture toughness (K_C) calculations were based on the crack length measurement of the radial crack pattern produced by Vickers indentations according to the formula estimated by Shetty et al. [20]. The fracture toughness values were derived from the average of 10 measurements. The samples were ground and polished by standard ceramographic methods and then etched in a Murakami's reagent consisting of $Fe_3[K(CN)_6]$ (10 g), KOH (10 g) and distilled water (100 ml) for 5 min to expose the grain boundary of WC; The WC grain size and Al_2O_3 particle size were estimated, respectively, by the linear intercept method. For each sample, at least three images were taken of the microstructure; in each image a minimum of five line segments were assessed.

3. Results and discussion

3.1. Powder characterization

The XRD patterns of commercial Al_2O_3 powders used in this study were shown in Fig. 1a. It indicated that the

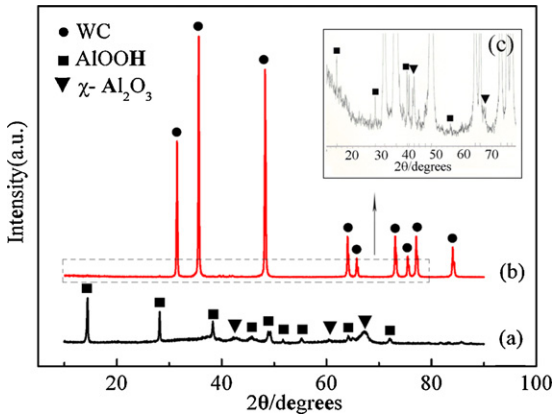

Fig. 1. XRD patterns of (a) commercial Al_2O_3 powders used in this study, (b) WC powders premixed with 40 vol.% commercial Al_2O_3 powders ball milled for 0 h, and (c) partially magnified XRD patterns of (b).

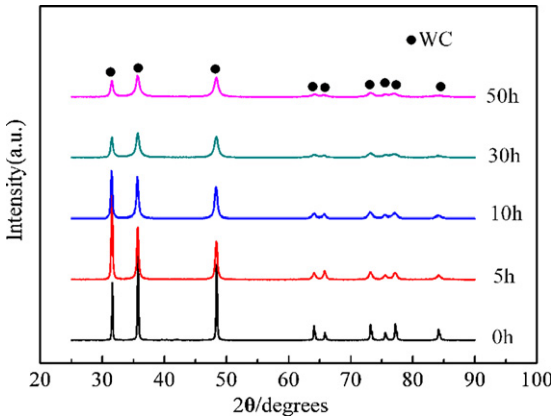

Fig. 2. XRD patterns of WC–40 vol.%Al_2O_3 powders ball-milled for different hours.

commercial Al_2O_3 powders were consisted of a great quantity of amorphous Al_2O_3 and trace amounts of AlOOH and χ-Al_2O_3. Fig. 1b shows the XRD patterns of WC powders premixed with 40 vol.% commercial Al_2O_3 powders ball milled for 0 h. The peaks of AlOOH and χ-Al_2O_3 were not observed in Fig. 1b due to the small content and their low intensity compared with that of WC. However, the partially magnified XRD pattern of Fig. 1b, as shown in Fig. 1c, confirms the existence of AlOOH and χ-Al_2O_3.

Fig. 2 shows the XRD patterns of WC–40 vol.%Al_2O_3 powders ball-milled for different hours. During the milling process, only peaks belonging to WC were observed, indicating that no composition changes took place, and phase transformation of AlOOH, χ-Al_2O_3 and amorphous Al_2O_3 did not occur. During the ball milling process, the AlOOH and χ-Al_2O_3 were refined and the particles were too small to be detected. With the increase of milling time, the XRD peaks of WC broadened and the intensity decreased in response to decreasing crystalline size, as well as increasing lattice strain.

From the secondary electron (SE) image of the WC–40 vol.%Al_2O_3 composites ball milled for 50 h, it can be seen that the powders were consisted of a mixture of fine and large grains of the product particles, as shown in Fig. 3a. The particle size varied from 46.67 to 573.33 nm in diameter. The bright

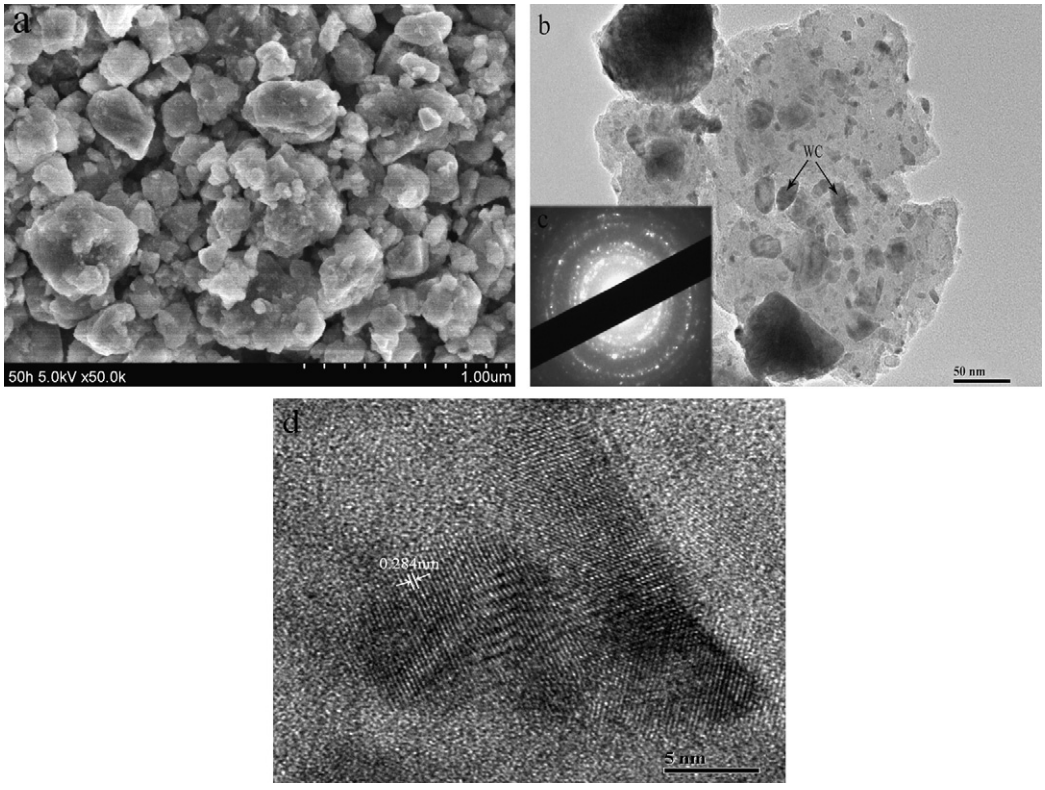

Fig. 3. (a) SEM, (b) BFI, (c) the corresponding SADP and (d) HRTEM micrograph of the WC–40 vol.%Al_2O_3 powders ball-milled for 50 h.

field images (BFI) of the end product are shown in Fig. 3b. Obviously, the dark grains and grey grains are WC and Al_2O_3. Fig. 3c shows the selected area diffraction pattern (SADP) of the end product taken at the middle of the micrograph. According to the XRD results shown in Fig. 1, there are amorphous Al_2O_3 and crystalline WC in the starting powder. From Fig. 2, it can be seen that the phase transformation and crystallization of the amorphous Al_2O_3 did not occur. So there should be still some amorphous Al_2O_3 existed in the milled powders. As shown in Fig. 3c, the diffuse diffraction rings indicates the existence of amorphous Al_2O_3 and the much stronger diffraction lines stands for the crystalline parts of WC. The internal structure of the powder end product was studied by HRTEM technique. The HRTEM micrograph of this product is presented in Fig. 3d. The deep black grain belongs to WC, as indicated by the lattice-fringe image (0.284 nm), which is oriented to the (0 0 1) plane.

3.2. Densification and phase analysis

Densification studies are carried out in both the hot pressing furnace as well as a dilatometer in N_2 atmospheric conditions. The relative density of WC–40 vol.%Al_2O_3 bulk composites after hot pressing at different temperature with varying holding time is shown in Fig. 4. It can be observed in Fig. 4 that, when the samples were sintered for a same holding time, the relative density of WC–40 vol.%Al_2O_3 bulk composite were enhanced with the increasing sintering temperature, while, when the samples were sintered at a same sintering temperature, the improvement of the relative density were recorded with a corresponding elongated holding time. The highest bulk density was 99.77% attained for the composite powder sintered at 1700 °C for 2 h. With the increasing temperature, the relative density is improved, bringing about the decrease of the amount of porosity, while the grain growth occurs (Figs. 8 and 9) and the Vickers hardness and fracture toughness decrease (Fig. 10). Thereby, it indicated that the degree of the deterioration to the Vickers hardness and fracture toughness caused by grain growth overweighs the enhancement contributed by the decreased amount of porosity.

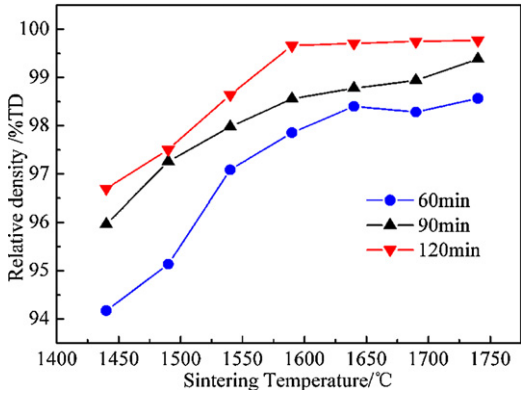

Fig. 4. The relative density of WC–40 vol.%Al_2O_3 bulk composites as a function of the sintering temperature and holding time.

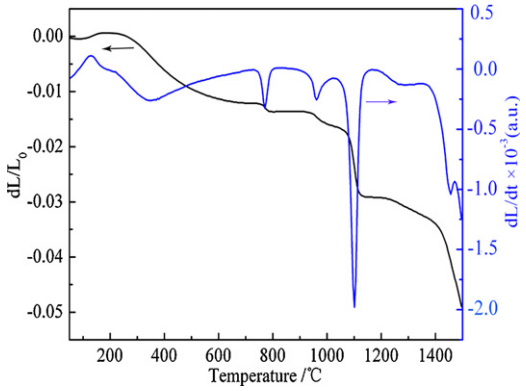

Fig. 5. Sintering shrinkage curve and its differential curve of as milled WC–40 vol.%Al_2O_3 powders.

The sintering shrinkage curve and its differential curve of as milled WC–40 vol.%Al_2O_3 powders were illustrated in Fig. 5. From Fig. 5, it can be seen that the shrinkage of WC–40 vol.%Al_2O_3 powder compact started at 227 °C and three obvious shrinkages in the temperature range from 753 °C to 784 °C, 940 °C to 1068 °C and 1068 °C to 1134 °C were observed with the increasing temperature. The maximum shrinkage rates of the shrinkage ranges were 769 °C, 961 °C and 1100 °C, respectively. The shrinkages of the powders are due to the effects of sintering and the phase transformation of the amorphous Al_2O_3, AlOOH and χ-Al_2O_3.

To investigate the actual sequence of phase transformation of WC–40 vol.%Al_2O_3 composites during hot pressing process, the premixed powders were sintered under load in vacuum atmosphere at predetermined temperatures of 769 °C, 961 °C, 1100 °C, 1540 °C and 1690 °C for 90 min, respectively. The X-ray patterns of the sintered samples are shown in Fig. 6.

From Fig. 6a, it can be seen that, when the premixed WC and commercial Al_2O_3 powders were sintered at 769 °C for 90 min, only the peaks of WC were observed, indicating that the shrinkage in the range from 227 °C to 784 °C was due to the loss of physically bonded water.

What exactly happens with the H_2O (the quantitative analysis) is difficult to measure during the hot pressing,

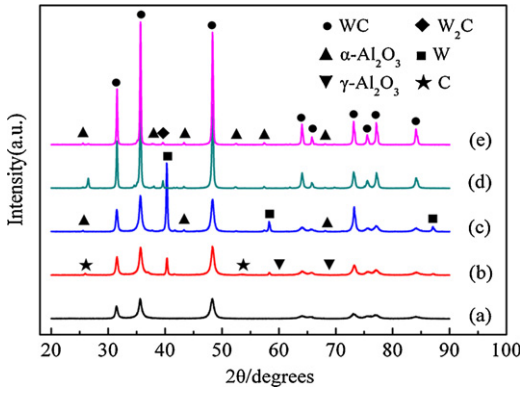

Fig. 6. XRD patterns of as milled powders sintered at (a) 769 °C for 90 min, (b) 961 °C for 90 min, (c) 1100 °C for 90 min, (d) 1540 °C for 90 min, and (e) 1690 °C for 90 min.

however, there is not a large amount of water vapor generated from the boehmite conversion, as can be deduced from the intensity of boehmite peaks in the XRD patterns shown in Fig. 1. Most of the water vapor from the boehmite conversion can escape from the composites, as there are continuous load and high temperature applied to the composites during hot pressing. Minor amount of the vapor become to be residual pores, the effects of which on the density is not obvious according to the high density of the composites.

The phases of the sample sintered at 961 °C for 90 min were C, WC, W and γ-Al_2O_3 (Fig. 6b). It is demonstrated that the shrinkage range of 940–1068 °C is attributed to the phase transformation of amorphous Al_2O_3 and AlOOH to γ and WC is decarburized seriously to C and W due to the low degree of vacuum during the sintering. The decarburization of WC to C and W is thought to proceed in the following three stages [21]:

$$2WC \rightarrow W_2C + C \quad (1)$$

$$W_2C + 1/2O_2 \rightarrow W_2(C, O) \quad (2)$$

$$W_2(C, O) \rightarrow 2W + CO \quad (3)$$

The first reaction is the classical one for WC decarburization. The degree of the powder's resistance to decarburization depends on the amount of WC or W_2C in the powder and on the oxygen content. The degree of vacuum during the sintering is low when the powders are hot pressing at 961 °C. As a result, there is a high concentration of oxygen in the furnace in addition to the oxides contained on the powders' surface. So the W_2C is decarburized into W.

All the transitional Al_2O_3 and amorphous Al_2O_3 were transformed to α-Al_2O_3 completely when the premixed powders were sintered at 1100 °C for 90 min, as shown in Fig. 6c. Phases of W are detected as well attribute to the decarburization of WC.

When the as milled powders were sintered at 1540 °C for 90 min, the decarburization of WC was not as serious as that of 1100 °C, however, a minor amount of C and W ($2\theta = 40.26^\circ$) besides WC and α-Al_2O_3 were observed in Fig. 6d. The existence of a minor amount of W could contribute to a metal particle toughening effect to the composites. This is one of the reasons for the high fracture toughness of the sample sintered at 1540 °C for 90 min. There are two possible reasons for the reduction of the content of W. On the one hand, when the sintering temperature is 1540 °C, the vacuum degree is higher than that of 1100 °C, the content of W decarburized from WC is decreased. On the other hand, the graphite die/punch set-up used during hot pressing is a potential carbon source that might recarburize the tungsten generated at lower temperature into WC by carbon interdiffusion.

The XRD pattern of as milled powders sintered at 1690 °C for 90 min is shown in Fig. 6e. Except for the peaks of WC, peaks belonging to α-Al_2O_3 and W_2C were identified. No other new phases could be identified even at 1690 °C, indicating that there is no reaction and no interface phase between WC and Al_2O_3 and they have good adopting characteristics. W_2C was formed during the sintering process. The WC and Al_2O_3 powders have been expected to contain surface oxides. When the powders are sintered under vacuum, the surface oxide is reduced. In this case, carbon is consumed in the reduction of surface oxide. Consequently, there is a lack of carbon to maintain the WC and WC is decarburized. W_2C phase forms due to the decarburization of WC during sintering [22]. Ma et al. [12] also observed the phenomenon of decarburization of WC phase and the formation of W_2C phase during the hot pressing process. With the high hardness and low Young's modulus [23], W_2C is generally thought to be a brittle phase harmful to the properties of the sintered composite, however, the formation and existence of W_2C is unavoidable.

3.3. Microstructure evolution

Polished microstructure of some representative samples is presented in Fig. 7a–e. The grey region contrasts Al_2O_3 and the bright region contrasts matrix WC. Fig. 7a–c reveal the microstructure of bulk samples sintered at 1440 °C, 1540 °C, 1640 °C for 90 min, respectively. It can be observed that grain growth behavior occurred with the increasing sintering temperature. There were larger Al_2O_3 and elongated faceted WC particles in the sample sintered at 1640 °C (Fig. 7c) than that in the samples sintered at 1440 °C and 1540 °C (Fig. 7a and b). From Fig. 7b, it can be seen that the particle size of both WC and Al_2O_3 was moderate, and Al_2O_3 homogeneously distributed in the WC matrix.

During the hot pressing process, the grain growth is unavoidable. At lower temperature, only surface diffusion promotes the grain growth. At higher temperature, grain growth is caused by the grain boundary migration, while grain boundary diffusion can still be activated causing enhanced density. Eq. (4) and (5) [24] can be used to describe the relationship between grain boundary mobility (B) and the coefficient of grain boundary diffusion (D_b).

$$B = D_b/RT \quad (4)$$

$$D_b = D_0 \exp(-Q_b/RT) \quad (5)$$

where B is the grain boundary mobility, D_b is the coefficient of grain boundary diffusion, D_0 is the constant of grain boundary diffusion, Q_b is the activation energy of the grain boundary diffusion, R is the universal gas constant, T is the sintering temperature. It can be seen that higher sintering temperature brings larger values of B and D_b, indicating the more quick grain growth speed. Accordingly, sintering temperature is one of the important factors influencing the microstructure and grain growth of the sintered composites.

The microstructure of the samples sintered at 1540 °C for 90 min, 60 min and 120 min were shown in Fig. 7b, d and e. Particle growth was observed with a corresponding increase of holding time. It indicates that holding time is another important factor affecting the grain growth. However, the particle size of the sample sintered at 1540 °C for 120 min was smaller than that of the sample sintered at 1640 °C for 90 min. It reveals that the influence of sintering temperature is much more obvious than that of holding time and sintering temperature is the

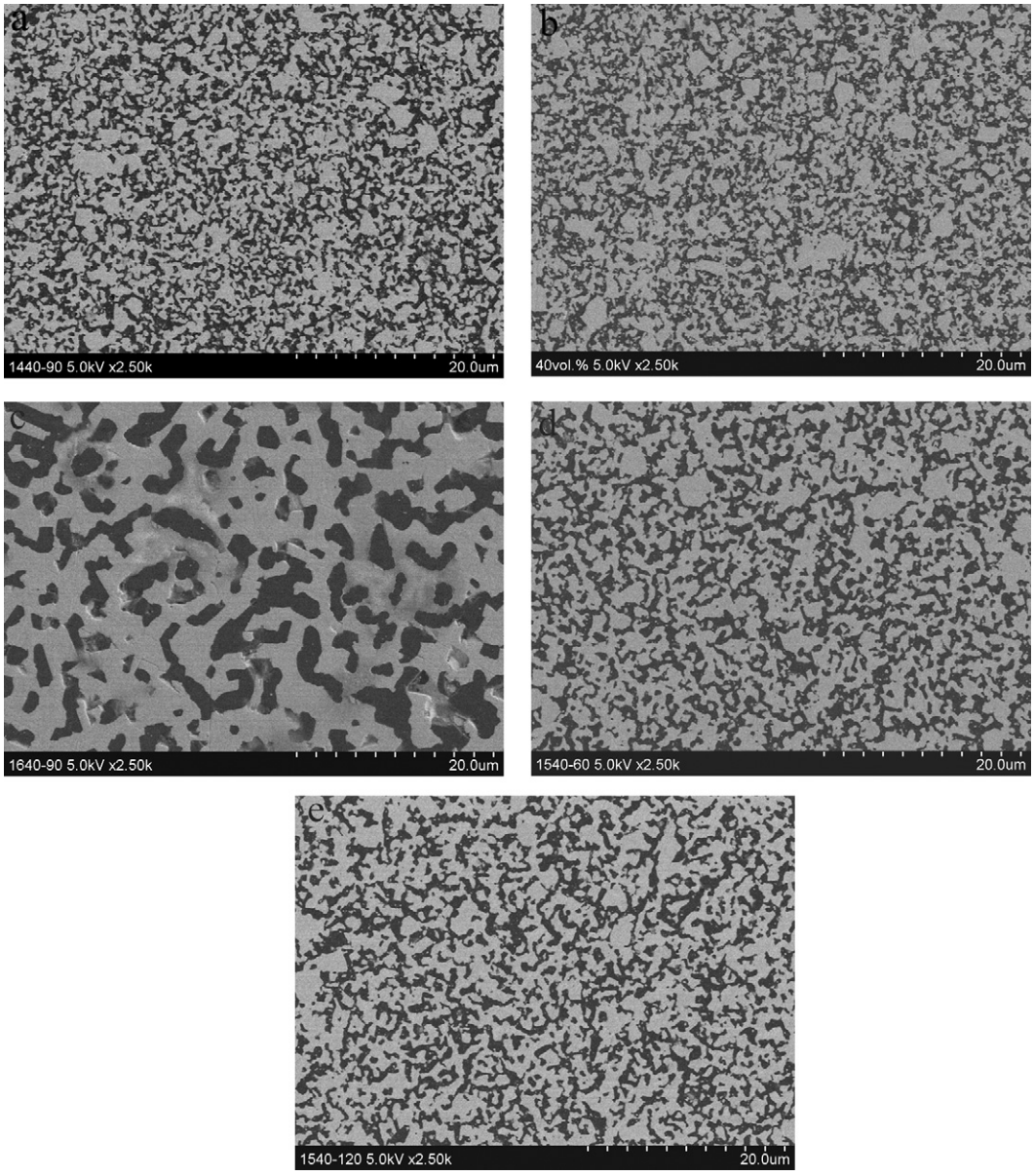

Fig. 7. FE-SEM of the polished WC–40 vol.%Al_2O_3 bulk composites sintered at (a) 1440 °C for 90 min, (b) 1540 °C for 90 min, (c) 1640 °C for 90 min, (d) 1540 °C for 60 min, and (e) 1540 °C for 120 min.

dominant factor of the sintering process, although both the sintering temperature and holding time are important factors of sintering process.

The characteristic microstructures of the polished and etched samples are shown in Fig. 8. A number of SEM photos similar to that of Fig. 8 were used to evaluate the grain size of WC and a number of FE-SEM images similar to that of Fig. 7 were used to evaluate the particle size of Al_2O_3. The particle size of Al_2O_3 and the grain size of WC as a function of the sintering temperature and holding time are shown in Fig. 9. For the holding time of 90 min, the particle size of Al_2O_3 increased from 1.35 μm to 3.47 μm while the grain size of WC increased from 2.13 μm to 4.35 μm when the temperature increased from 1440 °C to 1640 °C (Fig. 9a). When the temperature is 1540 °C, the particle size of Al_2O_3 increased from 1.59 μm to 2.1 μm while the grain size of WC increased from 2.19 μm to 3.7 μm when the holding time increased from 60 min to 120 min (as shown in Fig. 9b).

3.4. Effects of sintering temperature and holding time on the properties of the sintered samples

Vickers hardness and fracture toughness of WC–40 vol.%Al_2O_3 bulk composites as a function of sintering temperature and holding time were illustrated in Fig. 10a and b. It is shown that both the Vickers hardness and fracture toughness of WC–40 vol.%Al_2O_3 bulk composites increased until the appearance of the maximum values, and then followed a decreasing trend with the increasing sintering temperature no matter the holding time is 60 min, 90 min or 120 min. When the

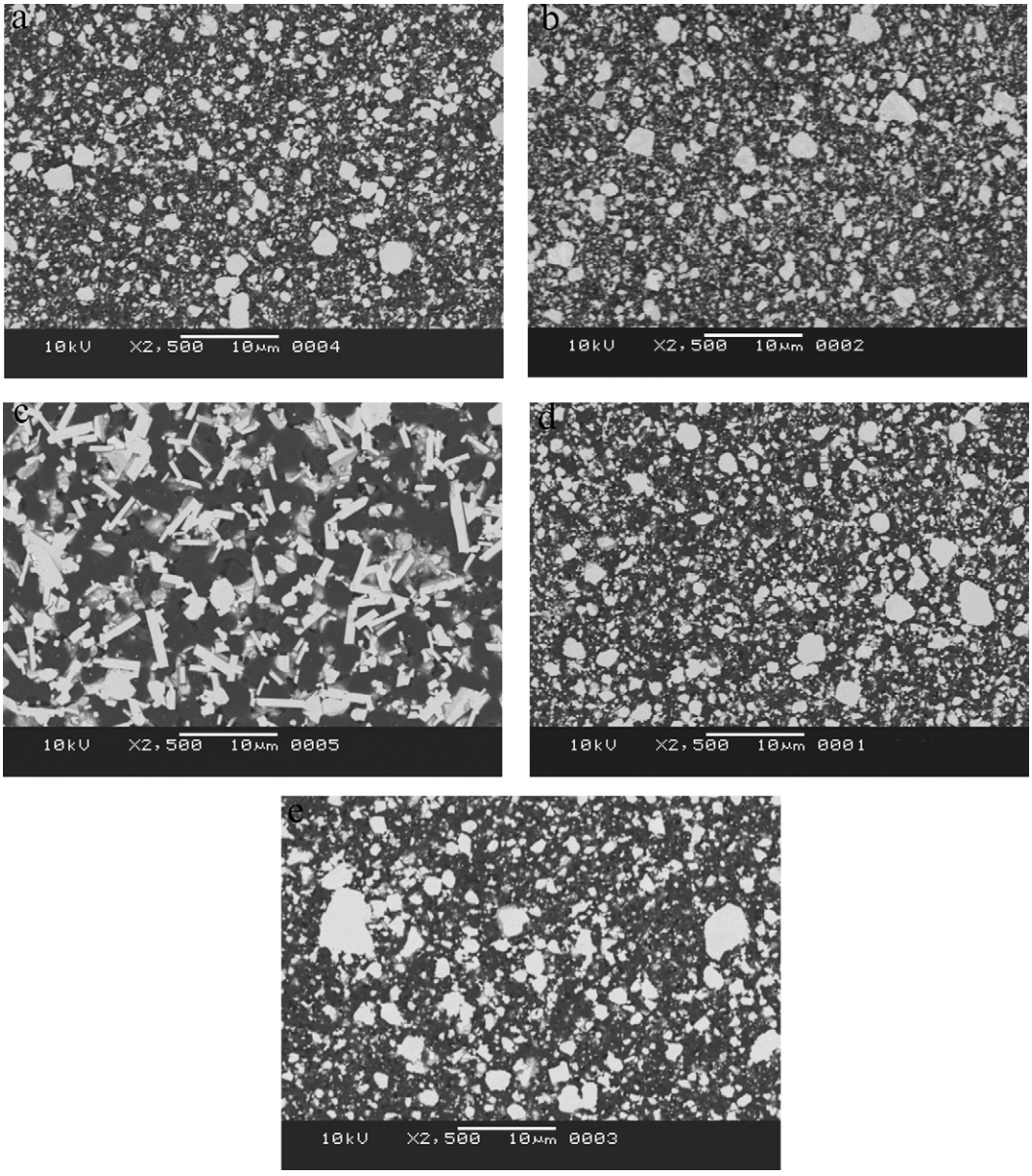

Fig. 8. SEM of the polished and etched WC–40 vol.%Al_2O_3 bulk composites sintered at (a) 1440 °C for 90 min, (b) 1540 °C for 90 min, (c) 1640 °C for 90 min, (d) 1540 °C for 60 min, and (e) 1540 °C for 120 min.

samples were sintered at 1540 °C for 90 min, the optimum hardness of 18.65 GPa was obtained. The excellent fracture toughness of 10.46 MPa $m^{1/2}$ was obtained in the samples sintered at 1590 °C for 90 min. Both the Vickers hardness and fracture toughness decreased obviously when the sample was sintered at 1640 °C.

As described in Fig. 4, when the temperature was over 1590 °C, the density of the samples increased slowly, especially when the holding time was 120 min, the density was almost constant. The samples sintered for 60 min have lower relative density and corresponding lower hardness compared with these sintered for 90 min, indicating that shorter holding time is not enough to get excellent properties. However, higher sintering temperature and a longer holding time of 120 min lead grains to growth quickly and irregularly, and induce the emergence of large Al_2O_3 and elongated WC particles, resulting in the decrease of the Vickers hardness and fracture toughness.

When the powders were sintered at lower temperature ($T < 1540$ °C) for a shorter holding time ($t < 90$ min), the density of the sample increased quickly while the grain size increased slightly (Fig. 9), so the influence of grain size is probably not obvious, the effect of the decreasing porosity is important. Both the Vickers hardness and fracture toughness increased with the decreasing porosity (the increasing density).

When the hot pressing temperature was higher ($T > 1540$ °C) and the holding time was longer ($t > 90$ min), the density of the samples increased slowly, while the particle size of Al_2O_3 and the grain size of WC increased quickly, as shown in Figs. 8 and 9. According to Fig. 10a and b, the Vickers hardness and fracture toughness decreases with the increasing temperature and holding

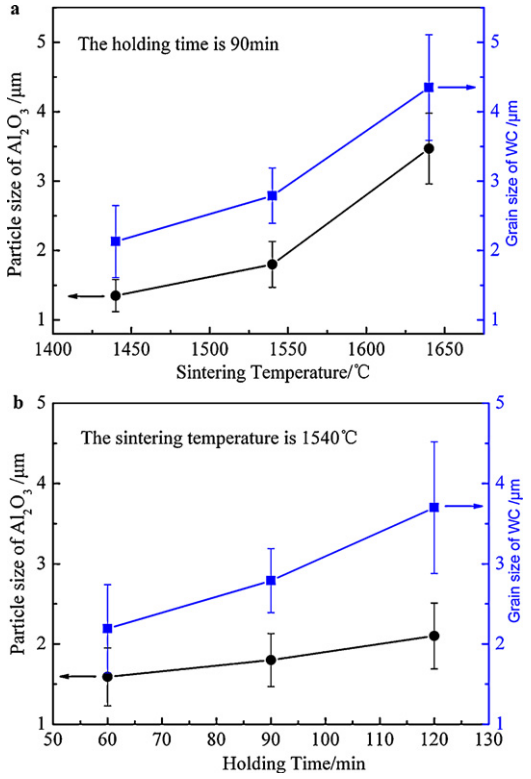

Fig. 9. The particle size of Al_2O_3 and the grain size of WC as a function of the sintering temperature and holding time.

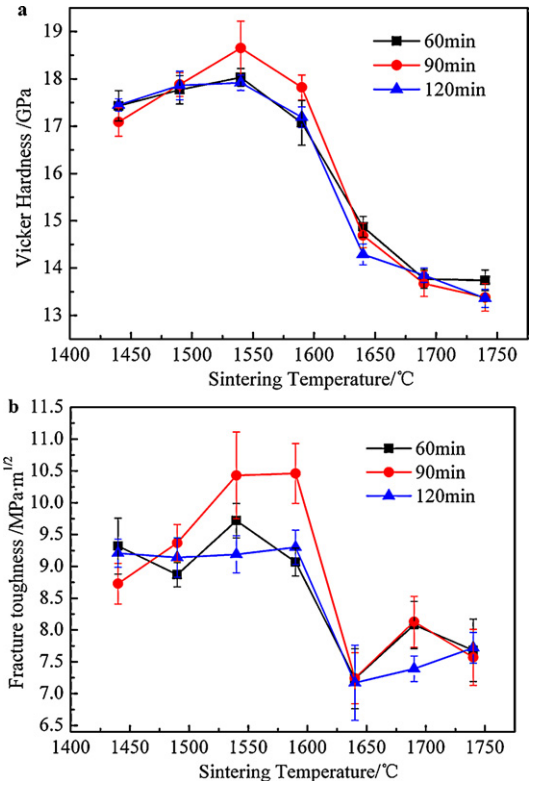

Fig. 10. (a) Vickers hardness, (b) Fracture toughness of WC–40 vol.%Al_2O_3 as a function of sintering temperature and holding time.

time, indicating that the lower hardness is due to the larger grain size and the contribution of coarse grains to the increase of fracture toughness attributed to the mechanisms of crack bridging and crack deflection is not significant.

It is presumably that the residual thermal stress field induced by the mismatch in the coefficients of thermal expansion (CTE) of the matrix and the particulate when the composite is cooled from the processing to the room temperature results in the variation of the mechanical properties of the sintered samples. For a finite volume fraction of particulates, the residual stress (P_i) for the particulates in the composites is [25]

$$P_i = 2\Delta\alpha\Delta T E_m/[(1+\upsilon_m)+2\beta(1-2\upsilon_p)E_m/E_p] \quad (6)$$

$$\Delta\alpha = \alpha_p - \alpha_m \quad (7)$$

$$\Delta T = T_p - T_r \quad (8)$$

where E_m, E_p are the Young's modulus of the matrix and the particulate; υ_m, υ_p are the Poisson's ratio of the matrix and the particulate; α_m, α_p are the CTEs of the matrix and the particulate; T_r is the room temperature and T_p denotes the processing temperature.

For the WC–Al_2O_3 composites, $\Delta\alpha > 0$, the radial tensile stress (σ_r) and the tangential compressive stress (σ_t) in the WC matrix around the Al_2O_3 particulates are

$$\sigma_r = P_i(r/R)^3 \quad (9)$$

$$\sigma_t = -1/2P_i(r/R)^3 \quad (10)$$

where r is the radius of the particulate; R is the distance away from the matrix/particulate interface.

It can be seen that because $\Delta\alpha > 0$, $\alpha_p > \alpha_m$, the shrinkage of the particulates during cooling is more obvious than that of the matrix, especially when the radius of a particulate is greater than the critical value, the particulate will be pulled off from the matrix by a large enough tensile stress (σ_r), inducing micro-cracks at the interface. If the interphase strength is high enough, tangential micro-cracks will be generated in the WC matrix surrounding the Al_2O_3 particulates [26]. Accordingly, when the powders were sintered at lower temperature ($T < 1540$ °C) for a shorter holding time ($t < 90$ min), the residual stress was small and the small residual stress could lead to the generation of branch and deflection of the cracks which were benefit to the increase of the fracture toughness. When the hot pressing temperature was higher ($T > 1540$ °C) and the holding time was longer ($t > 90$ min), both the particulate size and the residual stress reached a critical value, resulting in matrix micro-cracks that can be easily connected with each other upon external loading, reducing the fracture toughness of the material.

Evaluating the Vickers hardness and fracture toughness comprehensively, it reveals that the best sintering temperature is in the range of 1540–1590 °C and the optimum holding time is 90 min. According to the investigation of Huang et al. [19], pure WC could only be densified at 1900 °C for 2–4 min at 60 MPa. The addition of the commercial Al_2O_3 into WC matrix significantly reduces the sintering temperature required for achieving full densification.

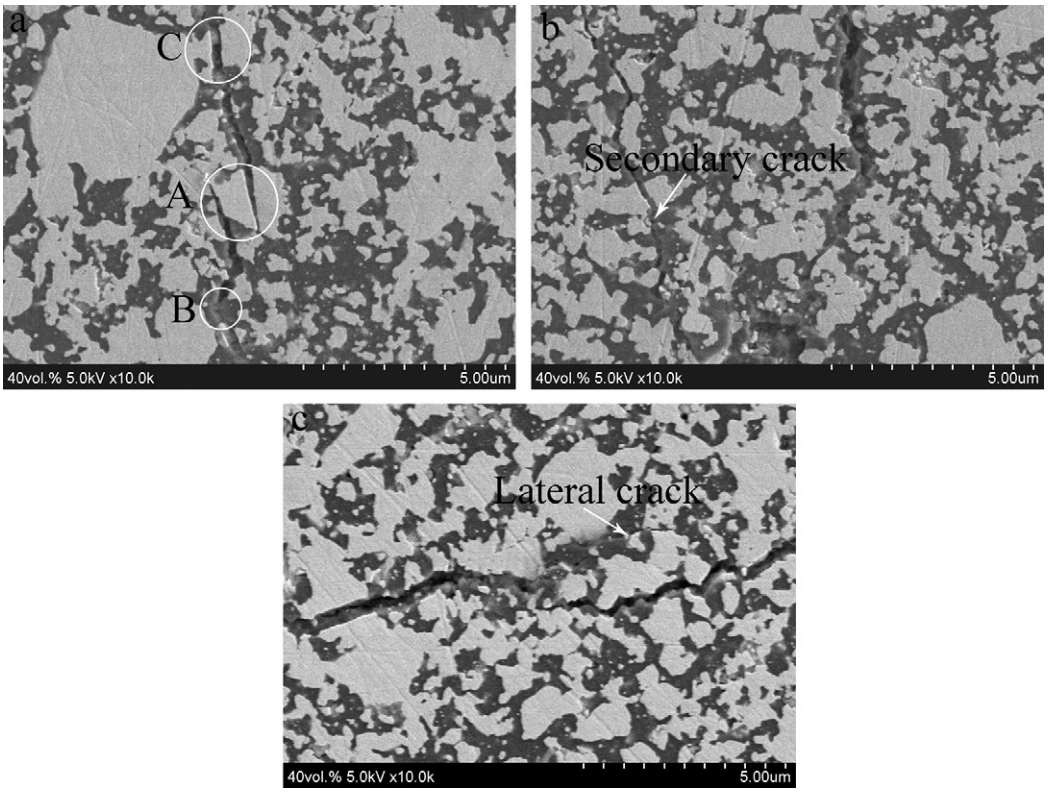

Fig. 11. FE-SEM of Vickers indentation crack extension path of WC–40 vol.% Al_2O_3 composites sintered at 1540 °C for 90 min: (a) crack bridging and crack deflection, (b) secondary crack, and (c) lateral crack.

3.5. Discussions on the toughening effects

The discussions on toughening effects are based on the study of the crack path microstructure. Fig. 11a–c reveals the Vickers indentation induced crack extension behavior in WC–40 vol.%Al_2O_3 composites. Fig. 11a illustrated the crack bridging by the WC matrix particles (region A), and the crack deflection when the crack tip reached Al_2O_3 particles (region B). Additionally, the crack propagation that broke the WC matrix particles (region C) can also be observed in Fig. 11a. Fig. 11b shows a secondary crack pattern during the indentation crack extension. Lateral crack and crack deflection both of which can provide restraining force for crack growth were indicated in Fig. 11c. In conclusion, crack bridging, crack deflections, the generation of secondary crack and lateral crack are dominant toughening mechanism in WC–40 vol.%Al_2O_3 composite.

Besides, it is interesting to consider the influence of phase transformation of the amorphous Al_2O_3 and transitional Al_2O_3 on the fracture toughness of WC–Al_2O_3 composites. As stated in Section 3.2, the amorphous Al_2O_3 and transitional Al_2O_3 transformed to α-Al_2O_3. The transformation of γ to α-Al_2O_3 occurs by nucleation and growth process [27], and rearrangement of particles occurs during the transformation [28]. Because of the difference in specific volume of boehmite (0.332 cm^3/g) and α-Al_2O_3 (0.25 cm^3/g), 24 vol.% porosity develops in the body after transformation [29]. A considerable amount of fine pores are redistributed throughout the compacts during sintering. Although there will be some water vapor generated from the boehmite conversion at the beginning stage of the sintering, the amount of water vapor will be small, and most of the water vapor can escape from the composites, only minor amount of the water vapor become residual pores as analyzed earlier, however, the effect of it on the density is not obvious according to the high density of the composites. Consequently, the obtained α-Al_2O_3 particles after transformation may be smaller than the particle size before transformation. As analyzed above, smaller size of secondary phase particulate brings benefit to the increase of the fracture toughness. So it can be deduced that there is a possibility that the phase transformation of the amorphous Al_2O_3 and transitional Al_2O_3 during sintering may be beneficial for the toughening of WC–Al_2O_3 composites. To confirm this opinion, further investigation is needed.

4. Conclusions

(1) WC–40 vol.%Al_2O_3 composite powders could be consolidated by hot pressing in the temperature range of 1440–1740 °C for 60 min, 90 min and 120 min under a pressure of 39.6 MPa.
(2) There is no phase transformation of premixed WC–40 vol.%Al_2O_3 powders during the high energy ball milling process, however, during the sintering process amorphous Al_2O_3, AlOOH and χ-Al_2O_3 are transformed to α-Al_2O_3 completely.

(3) Both the sintering temperature and holding time have remarkable influence on the microstructure and mechanical properties of WC–40 vol.%Al_2O_3 composite. With the increasing of sintering temperature and holding time, the relative density and particle size increase, while Vickers hardness and fracture toughness increased initially to the maximum values and then decreased. The WC–40 vol.%Al_2O_3 composites combine a relative density of 97.98% and an excellent Vickers hardness of 18.65 GPa with an acceptable fracture toughness of 10.43 MPa $m^{1/2}$ when hot pressed at 1540 °C for 90 min.
(4) The microstructural characterization of crack path revealed that crack bridging, crack deflection, the generation of secondary crack and lateral crack are main toughening mechanism in WC–40 vol.%Al_2O_3 composites.

Acknowledgements

The authors would like to acknowledge the financial support provided by Shanghai Leading Academic Discipline Project under project no: B602, and the support by the Nanomaterials Research Special Foundation of Shanghai Science and Technology Committee under grant no: 05nm05031.

References

[1] M. Sherif El-Eskandarany, M. Omori, M. Ishikuro, T.J. Konno, K. Takada, K. Sumiyama, T. Hirai, K. Suzuki, Synthesis of full-density nanocrystalline tungsten carbide by reduction of tungstic oxide at room temperature, Metall. Mater. Trans. A 27 (1996) 4210–4213.
[2] F.A. Deorsola, D. Vallauri, G.A. Ortigoza Villalba, B. De Benedetti, Densification of ultrafine WC-12Co cermets by pressure assisted fast electric sintering, Int. J. Refract. Met. Hard Mater. 28 (2010) 254–259.
[3] H.C. Kim, D.Y. Oh, I.J. Shon, Sintering of nanophase WC-15vol. %Co hard metals by rapid sintering process, Int. J. Refract. Met. Hard Mater. 22 (2004) 197–203.
[4] S. Imasato, T. Kei, K. Tetsunori, S. Shigeya, Properties of ultra-fine grain binderless cemented carbide 'RCCFN', Int. J. Refract. Met. Hard Mater. 13 (1995) 305–312.
[5] H.C. Kim, I.J. Shon, J.K. Yoon, J.M. Doh, Z.A. Munir, Rapid sintering of ultrafine WC-Ni cermets, Int. J. Refract. Met. Hard Mater. 24 (2006) 427–431.
[6] I.J. Shon, I.K. Jeong, I.Y. Ko, J.M. Doh, K.D. Woo, Sintering behavior and mechanical properties of WC-10Co WC-10Ni and WC-10Fe hard materials produced by high-frequency induction heated sintering, Ceram. Int. 35 (2009) 339–344.
[7] H.C. Kim, D.K. Kim, K.D. Woo, I.Y. Ko, I.J. Shon, Consolidation of binderless WC-TiC by high frequency induction heating sintering, Int. J. Refract. Met. Hard Mater. 26 (2008) 48–54.
[8] O. Malek, B. Lauwers, Y. Perez, P.D. Baets, J. Vleugels, Processing of ultrafine ZrO_2 toughened WC composites, J. Eur. Ceram. Soc. 29 (2009) 3371–3378.
[9] S.G. Huang, O. Van der Biest, J. Vleugels, Pulsed electric current sintered Fe_3Al bonded WC composites, Int. J. Refract. Met. Hard Mater. 27 (2009) 1019–1023.
[10] M.L. Zhang, S.G. Zhu, J. Ma, C.X. Wu, Preparation of WC/MgO composite nanopowders by high energy reactive ball milling and their plasma activated sintering, Powder Metall. Met. Ceram. 47 (2008) 9–10.
[11] C.X. Wu, S.G. Zhu, J. Ma, M.L. Zhang, Synthesis and formation mechanisms of nanocomposite WC-MgO powders by high-energy reactive milling, J. Alloys Compd. 478 (2009) 615–619.
[12] J. Ma, S.G. Zhu, P. Di, Y. Zhang, Influence of La_2O_3 addition on hardness flexural strength and microstructure of hot-pressing sintered WC-MgO bulk composites, Mater. Des. 32 (2011) 2125–2129.
[13] Holleckh, Material selection for hard coatings, J. Vac. Sci. Technol. A-Vacuum surf. Films 6 (4) (1986) 2661–2669.
[14] M. Sherif, El-Eskandarany, Fabrication and characterizations of new nanocomposite WC/Al_2O_3 materials by room temperature ball milling and subsequent consolidation, J. Alloys Compd. 391 (2005) 228–235.
[15] E.M.J.A. Pallone, D.R. Martin, R. Tomasi, W.J. Botta Filho, Al_2O_3-WC synthesis by high-energy reactive milling, Mater. Sci. Eng. A 464 (2007) 47–51.
[16] M. Sakaki, M.Sh. Bafghi, J. Vahdati Khaki, Q. Zhang, F. Saito, Effect of the aluminum content on the behavior of mechanochemical reactions in the WO_3-C-Al system, J. Alloys Compd. 480 (2009) 824–829.
[17] M. Sakaki, M.S. Bafghi, J. Vahdati Khaki, Q. Zhang, F. Saito, Control of carbon loss during synthesis of WC powder through ball milling of WO_3-C-2Al mixture, J. Alloys Compd. 486 (2009) 486–491.
[18] H. Endo, M. Ueki, Hot-pressing and pressureless sintering of WC-Al_2O_3 ceramic composites, Trans. Mat. Res. Soc. 16B (1994) 819–822.
[19] S.G. Huang, K. Vanmeensel, O. Van der Biest, J. Vleugels, Pulsed electric current sintering and characterization of ultrafine Al_2O_3–WC composites, Mater. Sci. Eng. A 527 (2010) 584–589.
[20] D.K. Shetty, I.G. Wright, P.N. Mincer, A.H. Clauer, Indentation fracture of WC-Co cermets, J. Mater. Sci. 20 (1985) 1873–1882.
[21] M.E. Vinayo, F. Kassabji, J. Guyonnet, P. Fauchais, Plasma sprayed WC-Co coatings: influence of spray conditions (atmospheric and low pressure plasma spraying) on the crystal structure, porosity, and hardness, J. Vac. Sci. Technol. A 3 (6) (1985) 2483–2489.
[22] S.I. Cha, S.H. Hong, Microstructures of binderless tungsten carbides sintered by spark plasma sintering process, Mater. Sci. Eng. A 356 (2003) 381–389.
[23] H. Taimatsu, S. Sugiyama, Y. Kodaira, Synthesis of W_2C by reactive hot pressing and its mechanical properties, Mater. Trans. 49 (2008) 1256–1261.
[24] G.X. Hu, X. Cai, Y.H. Rong, Fundamental of Materials Science, Publisher of Shanghai Jiaotong University, 2006.
[25] J. Selsing, Internal stress in ceramics, J. Am. Ceram. Soc. 71 (8) (1961) 419–421.
[26] Y. Huang, C.A. Wang, Multiphase Composite Ceramics with High Performance, Publisher of Tsinghua University, 2008.
[27] P.A. Badkar, J.E. Bailey, The mechanism of simultaneous sintering and phase transformation in alumina, J. Mater. Sci. 11 (1976) 1794–1806.
[28] C. Legros, C. Carry, P. Bowen, H. Hofmann, Sintering of a transition Alumina: effects of phase transformation powder characteristic and thermal cycle, J. Eur. Ceram. Soc. 19 (1999) 1967–1978.
[29] C. Kaya, J.Y. He, X. Gu, E.G. Butler, Nanostructure ceramic powders by hydrothermal synthesis and their applications, Microporous Mesoporous Mater. 54 (2002) 37–49.